
Hierarchical Graph Pooling Based on Minimum Description Length

Jan von Pichowski  Christopher Blöcker  Ingo Scholtes 

Chair of Machine Learning for Complex Networks
Centre for Artificial Intelligence and Data Science (CAIDAS)
Julius-Maximilians-Universität Würzburg, Germany
{jan.pichowski, christopher.bloecker, ingo.scholtes}@uni-wuerzburg.de

Abstract

Graph pooling is an essential part of deep graph representation learning. We introduce *MapEqPool*, a principled pooling operator that takes the inherent hierarchical structure of real-world graphs into account. *MapEqPool* builds on the map equation, an information-theoretic objective function for community detection based on the minimum description length principle which naturally implements Occam’s razor and balances between model complexity and fit. We demonstrate *MapEqPool*’s competitive performance with an empirical comparison against various baselines across standard graph classification datasets.

1 Introduction

Graph neural networks (GNNs) are applied to graph-structured data from various domains to address diverse research questions, for example analysing scientific collaborations [1] and understanding molecule properties [2] such as mutagenicity [3]. An important application in graph representation learning is graph classification which requires reducing, or coarsening, a graph to an embedding vector representing its properties for classification.

Links in real-world graphs often form according to some stochastic process [4–6], typically not directly observable, connecting nodes in clusters, also called communities [7, 8], such as groups of friends in social networks [9] or functional or secondary groups amongst molecules [2]. Communities can be obtained using inferential or descriptive methods [10–16], differing in how precisely they characterise what constitutes communities [8]. Some deep learning approaches are based on learning those characteristics to obtain a clustering, which can then be used to coarsen graphs for downstream tasks [17, 18].

Ying et al. [18] suggest coarsening graphs by repeatedly applying the same clustering method, reflecting the multiple cluster levels found in many real-world graphs [19, 20]. While such stacking enables end-to-end learning of multilevel clusters based on a differentiable model, it neglects the interdependencies between different clustering levels. Specifically, stacking learners only considers clusters in a bottom-up fashion because it optimises the clustering objective for clusters at lower levels before moving on to higher levels. Consequently, the clusters at higher levels cannot influence the lower levels, see Figure 1(a-b) for an example. In contrast, several community-detection objective functions jointly consider the clusterings across different hierarchical levels, including the nested stochastic block model [21] and the multilevel map equation [22]. However, to the best of our knowledge, no deep graph pooling method based on such a joint notion of hierarchical clusters has been proposed to date.

To address this gap, we propose *MapEqPool*, a hierarchical pooling operator that jointly optimises the clusterings across different hierarchical levels. Our contributions are as follows:

- (i) We derive a multilevel clustering objective from the map equation to learn hierarchical pooling operators jointly optimised for multiple clustering levels. Specifically, in contrast to other approaches where only coarser levels depend on finer ones, we consider all levels together.

- (ii) Following the minimum description length principle, our approach implements Occam’s razor, automatically selecting the optimal number of clusters and balancing between model complexity and fit. Explicit regularisation, while essential for other approaches, is superfluous in our case.
- (iii) We empirically verify the utility of *MapEqPool*’s unified clustering formulation by comparing it to various baseline methods in a range of standard benchmarks from different domains.

Different from previous works, we introduce a truly hierarchical pooling method and the first application of the map equation as a pooling operator, following a recent direction of incorporating principled statistical methods [23] in general, and the map equation in particular into deep graph learning [24].

2 Related Work

Graph Clustering. Graph clustering, also known as community detection, seeks to partition graphs into clusters, or communities, of “similar” nodes [8]. Many methods for graph clustering exist, including the stochastic block model [25], modularity [26], k-cuts [27], and the map equation [14]. Several of those methods were adapted for deep learning: Bianchi et al. [17] learn clusters by optimising a min-cut objective, Tsitsulin et al. [28] follow the modularity objective, and Blöcker et al. [24] adapt the map equation. Ying et al. [18] follow a heuristic that seeks to group nearby nodes together while each node should belong to only one cluster.

Graph Pooling. Graph pooling provides a way to obtain a coarse-grained graph representation. Mean and sum pooling coarsen graphs in a single step. Attention-based techniques only retain the information for important nodes [29, 30]. Clustering-based methods adopt the notion of clusters as defined by heuristics [18] or concepts such as minimum cuts [17]. They learn a cluster assignment with a loss objective encoding the specific concept and merge nodes with the same assignment.

Any shallow pooling approach can be stacked for hierarchical clustering [18], however, stacking does not consider the interdependencies between clusters at different levels because the clustering objective is optimised for finer levels before the coarser levels are considered. Here, we remedy this issue by proposing a hierarchical pooling approach that jointly optimises the clusters across multiple levels (see Figure 1).

Map Equation and Neuomap. The map equation [6, 14] is an information-theoretic objective function for community detection based on the description of random walks. It implements Occam’s razor by following the minimum description length principle [31, 32], thereby automatically balancing model complexity with goodness of fit. Given a set of communities, the map equation analytically computes the expected number of bits per step—the so-called *codelength*—that would be required to encode the trajectory of a random walker. Detecting communities with the map equation is NP-hard and can be done with Infomap, a stochastic and greedy search algorithm [6, 33]. Recently, Blöcker et al. [24] adapted the map equation as a soft clustering objective for optimisation with GNNs and gradient descent, however, they did not consider hierarchical clustering or pooling.

3 Background: Multilevel Map Equation

Let $G = (V, E)$ be a graph, possibly weighted and/or directed, let w_{uv} denote the weight on link (u, v) , and let M be a partition of the nodes into modules. Further, let \mathbf{T} be G ’s transition matrix with $\mathbf{T}_{uv} = w_{uv} / \sum_v w_{uv}$. The nodes’ ergodic visit rates can be computed with a power iteration to solve the set of equations $p_v = \sum_u p_u t_{uv}$ in strongly-connected graphs [6]; otherwise, PageRank [34] or smart teleportation [35] can be used. The two-level map equation calculates M ’s codelength as

$$L(M) = q_{\curvearrowright} H(Q) + \sum_{m \in M} p_m^{\circ} H(P_m). \quad (1)$$

Here, $q_{\curvearrowright} = \sum_{m \in M} q_m^{\wedge}$ is the overall module entry rate, q_m^{\wedge} is module m ’s entry rate; $p_m^{\circ} = q_m^{\wedge} + \sum_{u \in m} p_u$ is the usage rate for module m , and q_m° is module m ’s exit rate. Further, H is the Shannon entropy, $Q = \{q_m^{\wedge}/q_{\curvearrowright} \mid m \in M\}$ is the set of normalised module entry rates, and $P_m = \{q_m^{\wedge}/p_m^{\circ}\} \cup \{p_u/p_m^{\circ} \mid u \in m\}$ is the set of normalised node visit and exit rates for m . For more details and a complete example, see Appendix A. The multilevel map equation generalises the map equation to hierarchical partitions through recursion [6, 22],

$$L(M) = q_{\curvearrowright} H(Q) + \sum_{m \in M} L(m). \quad (2)$$

4 Hierarchical Pooling with Multilevel Map Equation Loss

In analogy to expanding the two-level map equation [14], the ℓ -level map equation can be written as

$$L(M)^{(\ell)} = q_{\curvearrowright} \log q_{\curvearrowright} \quad (3)$$

$$+ \sum_{m^{(1)} \in M} [-q_{m^{(1)}}^{\curvearrowleft} \log q_{m^{(1)}}^{\curvearrowleft} - q_{m^{(1)}}^{\curvearrowright} \log q_{m^{(1)}}^{\curvearrowright} + q_{m^{(1)}}^{\circ} \log q_{m^{(1)}}^{\circ}] \quad (4)$$

$$+ \sum_{m^{(1)} \in M} \sum_{m^{(2)} \in m^{(1)}} [-q_{m^{(2)}}^{\curvearrowleft} \log q_{m^{(2)}}^{\curvearrowleft} - q_{m^{(2)}}^{\curvearrowright} \log q_{m^{(2)}}^{\curvearrowright} + q_{m^{(2)}}^{\circ} \log q_{m^{(2)}}^{\circ}] \quad (5)$$

$$+ \dots \quad (6)$$

$$+ \sum_{m^{(1)} \in M} \sum_{m^{(2)} \in m^{(1)}} \dots \sum_{u \in m^{(\ell-1)}} -p_u \log p_u \quad (7)$$

Appendix B shows in detail how to obtain the equation. Here, we adapt this multilevel map equation to derive a hierarchical clustering objective and optimise it through gradient descent. We use our clustering objective as a loss term to indirectly optimise the soft cluster assignments $\mathbf{S} = \text{softmax}(\text{GNN}_{\theta}(\mathbf{A}, \mathbf{X}))$ through the GNN’s parameters θ . In the following, we fix the number of levels to $\ell = 3$ in analogy to [18], however, the equations can be expanded to more levels. We learn two soft cluster-assignment matrices $\mathbf{S}_m \in \mathbb{R}^{n \times m}$ and $\mathbf{S}_M \in \mathbb{R}^{m \times M}$ that pool the $n = |V|$ nodes first into m sub-modules and then the m sub-modules further into M modules.

The flow matrix $\mathbf{F}_{uv} = p_u \mathbf{T}_{uv}$ encodes the flow between each pair of nodes [24]. For soft clusters, we weigh the node visit rates p_u according to the nodes’ share in the given clusters: $\mathbf{p}_{uij} = p_u \mathbf{S}_{m_{ui}} \mathbf{S}_{M_{ij}}$. The flow $\mathbf{C}_m = \mathbf{S}_m^{\top} \mathbf{F} \mathbf{S}_m \odot \mathbf{S}_M \mathbf{S}_M^{\top}$ between clusters, derived from the sub-module assignments \mathbf{S}_m , is pooled from the flow matrix \mathbf{F} . At the sub-module level, we remove the flow between (super)-modules M with an element-wise multiplication. For larger ℓ , this needs to be done at all intermediate levels. The flow $\mathbf{C}_M = \mathbf{S}_M^{\top} \mathbf{S}_m^{\top} \mathbf{F} \mathbf{S}_m \mathbf{S}_M$ for the top-level modules is obtained through recursive pooling.

We obtain the module entry and exit rates from the cluster flow matrices \mathbf{C}_m and \mathbf{C}_M . The module flows for the sub-modules are weighted according to the soft clusters in the (super)-modules M :

$$\mathbf{q}_{m'_{ij}}^{\curvearrowleft} = [\mathbf{C}_m \mathbf{1}_{|m|} - \text{diag}(\mathbf{C}_m)]_{ij} \mathbf{S}_{M_{ij}} \quad \mathbf{q}_m^{\curvearrowleft} = \mathbf{C}_M \mathbf{1}_{|M|} - \text{diag}(\mathbf{C}_M) \quad (8)$$

$$\mathbf{q}_{m'_{ij}}^{\curvearrowright} = [\mathbf{C}_m^{\top} \mathbf{1}_{|m|} - \text{diag}(\mathbf{C}_m)]_{ij} \mathbf{S}_{M_{ij}} \quad \mathbf{q}_m^{\curvearrowright} = \mathbf{C}_M^{\top} \mathbf{1}_{|M|} - \text{diag}(\mathbf{C}_M) \quad (9)$$

$$\mathbf{q}_{m'_{ij}}^{\circ} = [\mathbf{q}_m^{\curvearrowleft} + \mathbf{S}_m^{\top} \mathbf{p}_u^{\curvearrowleft}]_{ij} \mathbf{S}_{M_{ij}} \quad \mathbf{q}_m^{\circ} = \mathbf{q}_m^{\curvearrowleft} + \mathbf{S}_m^{\top} \mathbf{q}_m^{\curvearrowright} \quad (10)$$

Finally, we obtain the hierarchical (three-level) loss $L(\mathbf{A}, \mathbf{S}_M, \mathbf{S}_m)$ with $q_{\curvearrowright} = 1 - \text{Tr}(\mathbf{C}_M)$:

$$L(\mathbf{A}, \mathbf{S}_M, \mathbf{S}_m)^{(3)} = q_{\curvearrowright} \log q_{\curvearrowright} + \sum_{j \in M} [-\mathbf{q}_m^{\curvearrowleft} \log \mathbf{q}_m^{\curvearrowleft} - \mathbf{q}_m^{\curvearrowright} \log \mathbf{q}_m^{\curvearrowright} + \mathbf{q}_m^{\circ} \log \mathbf{q}_m^{\circ}]_j \quad (11)$$

$$+ \sum_{i \in m, j \in M} [-\mathbf{q}_{m'_{ij}}^{\curvearrowleft} \log \mathbf{q}_{m'_{ij}}^{\curvearrowleft} - \mathbf{q}_{m'_{ij}}^{\curvearrowright} \log \mathbf{q}_{m'_{ij}}^{\curvearrowright} + \mathbf{q}_{m'_{ij}}^{\circ} \log \mathbf{q}_{m'_{ij}}^{\circ}]_{ij} + \sum_{u \in V, i \in m, j \in M} [-\mathbf{p} \log \mathbf{p}]_{uij} \quad (12)$$

The above loss encodes the three-level map equation, which, different from other deep clustering methods, does not require explicit regularisation to prevent trivial solutions [24].

We obtain \mathbf{S}_m and \mathbf{S}_M through an MLP that maps the node embedding to those soft cluster assignments. The node features \mathbf{X} and adjacency matrix \mathbf{A} are pooled twice as follows:

$$\mathbf{A}^{(1)} = \mathbf{S}_m^{\top} \mathbf{A} \mathbf{S}_m \quad \mathbf{X}^{(1)} = \mathbf{S}_m^{\top} \mathbf{X} \quad \mathbf{A}^{(2)} = \mathbf{S}_M^{\top} \mathbf{A}^{(1)} \mathbf{S}_M \quad \mathbf{X}^{(2)} = \mathbf{S}_M^{\top} \mathbf{X}^{(1)} \quad (13)$$

We call our hierarchical pooling operator *Hierarchical Map Equation Pooling* (*MapEqPool*) and learn it by optimising the multilevel loss $L(\mathbf{A}, \mathbf{S}_M, \mathbf{S}_m)$ with the model architecture shown in Figure 1(c).

5 Experimental Evaluation

We compare our pooling method, **MapEqPool**, against **DiffPool** [18], **MinCutPool** [17], **SAG-Pool** [29], **TopK** [30] and global **Mean** pooling. Additionally, we introduce a model **MapEqPool^S** that stacks two shallow Neuromap pooling layers and sums their losses as done in the other baselines.

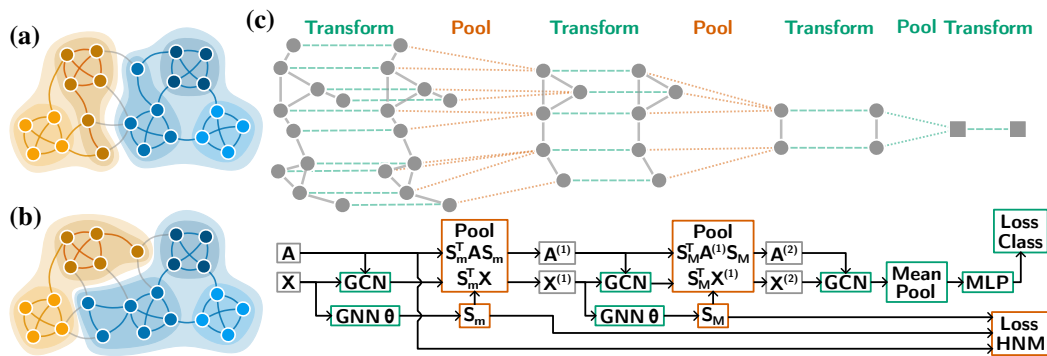


Figure 1: (a-b) All tested clustering methods agree that the clusters in (a) have lower loss and, thus, are better than those in (b). However, the stacked pooling operators consider the lower-level clusters in (b) superior to the lower-level clusters in (a). Because they cannot consider the coarser clusters during the first step, they cannot obtain the overall better assignment shown in (a). In contrast, our approach optimises the total assignment and returns (a) as the better solution, choosing a worse solution at the lower level for an overall better solution. See Appendix C for the methods’ loss values. (c) Our multilevel pooling architecture. The blocks shown in green are the same across all methods, the orange blocks differ. While the baselines rely on summing two separate losses, our approach unifies both pooling operations in one joint loss.

We use the same neural network architecture for all experiments: It consists of three graph convolution layers, each separated by one pooling layer. Afterwards, the remaining nodes are pooled with mean pooling, followed by a linear layer to solve the classification task. We evaluate the models with 10-fold stratified cross-validation and select the best epoch based on a validation set that is split from the training folds (see Appendix D for more training details).

We select data sets from different domains typically used for evaluating pooling methods: *MUTAG* [3], *PROTEINS* [2], and *DD* [36] contain molecules, *REDDIT-B* [1], *REDDIT-5K* [1] contains social interactions, and *COLLAB* [1] contains collaboration networks. The data sets vary in size from 188 to 5000 graphs and the average node count varies from 17.93 to 508.52. *COLLAB* and *REDDIT-5K* have multi-class classification tasks whereas the others are binary (see Appendix E for details).

Table 1: Balanced accuracy of MapEqPool and five baselines in our empirical evaluation. We mark the best results. Appendix D presents additional metrics.

| Method | MUTAG | PROTEINS | COLLAB | DD | REDDIT-B | REDDIT-5K |
|------------------------|---------------------|---------------------|---------------------|---------------------|---------------------|---------------------|
| Global Mean | 80.99 ± 10.04 | 67.18 ± 4.31 | 64.61 ± 1.41 | 69.82 ± 3.65 | 65.43 ± 3.79 | 36.99 ± 4.65 |
| MinCutPool | 76.13 ± 11.63 | 73.10 ± 5.05 | 65.57 ± 3.51 | 76.22 ± 2.76 | 77.28 ± 4.00 | 47.14 ± 1.69 |
| DiffPool | 71.72 ± 12.52 | 73.22 ± 4.03 | 64.27 ± 3.52 | 74.15 ± 4.24 | 74.48 ± 4.77 | 47.54 ± 2.11 |
| TopK | 63.39 ± 15.55 | 65.35 ± 6.51 | 60.02 ± 2.72 | 75.53 ± 2.79 | 77.86 ± 3.10 | 47.65 ± 2.24 |
| SAGPool | 75.47 ± 9.57 | 62.57 ± 7.80 | 56.75 ± 5.07 | 72.93 ± 2.39 | 79.36 ± 3.35 | 45.54 ± 2.88 |
| MapEqPool ^S | 79.67 ± 10.13 | 71.95 ± 4.00 | 68.83 ± 3.55 | 76.33 ± 3.32 | 77.60 ± 2.80 | 45.65 ± 3.64 |
| MapEqPool | 81.40 ± 6.70 | 73.41 ± 4.44 | 65.43 ± 3.06 | 78.31 ± 2.94 | 77.74 ± 3.49 | 46.86 ± 1.80 |

6 Conclusion

We proposed *MapEqPool*, a hierarchical graph pooling operator based on the map equation. Different from previous works, we introduce a multilevel pooling objective that jointly optimises the clusters across hierarchical levels instead of merely stacking non-hierarchical clustering operators. Because our loss follows the minimum description length principle, it automatically selects the optimal number of clusters and balances between model complexity and fit without requiring explicit regularisation which was essential in previous works. In an empirical evaluation on six common graph classification datasets, we showed that *MapEqPool* performs competitively against popular baselines.

Despite these contributions, our work raises open questions: Following previous works, we fixed the number of hierarchical levels to three, however, our approach is not limited to a fixed depth but can be generalised to an arbitrary number of levels. This poses two challenges: (1) When the targeted number of levels is larger than the number of levels present in the graph, the map equation must account for singleton clusters. For simplicity, we did not consider this in our restricted case. (2) More importantly, deeper pooling results in deeper GNNs, which makes their training more challenging.

References

- [1] Pinar Yanardag and S.V.N. Vishwanathan. Deep graph kernels. In *Proceedings of the 21th ACM SIGKDD International Conference on Knowledge Discovery and Data Mining*, KDD '15, pages 1365–1374. Association for Computing Machinery. ISBN 978-1-4503-3664-2. doi: 10.1145/2783258.2783417. URL <https://dl.acm.org/doi/10.1145/2783258.2783417>.
- [2] Karsten M. Borgwardt, Cheng Soon Ong, Stefan Schönauer, S. V. N. Vishwanathan, Alex J. Smola, and Hans-Peter Kriegel. Protein function prediction via graph kernels. 21:i47–i56. ISSN 1367-4803. doi: 10.1093/bioinformatics/bti1007. URL <https://doi.org/10.1093/bioinformatics/bti1007>.
- [3] Asim Kumar Debnath, Rosa L. Lopez de Compadre, Gargi Debnath, Alan J. Shusterman, and Corwin Hansch. Structure-activity relationship of mutagenic aromatic and heteroaromatic nitro compounds. correlation with molecular orbital energies and hydrophobicity. 34(2):786–797. ISSN 0022-2623. doi: 10.1021/jm00106a046. URL <https://doi.org/10.1021/jm00106a046>. Publisher: American Chemical Society.
- [4] M. E. J. Newman. Clustering and preferential attachment in growing networks. *Phys. Rev. E*, 64:025102, Jul 2001. doi: 10.1103/PhysRevE.64.025102. URL <https://link.aps.org/doi/10.1103/PhysRevE.64.025102>.
- [5] Alexei Vázquez. Growing network with local rules: Preferential attachment, clustering hierarchy, and degree correlations. *Phys. Rev. E*, 67:056104, May 2003. doi: 10.1103/PhysRevE.67.056104. URL <https://link.aps.org/doi/10.1103/PhysRevE.67.056104>.
- [6] Jelena Smiljanić, Christopher Blöcker, Anton Holmgren, Daniel Edler, Magnus Neuman, and Martin Rosvall. Community detection with the map equation and infomap: Theory and applications, 2023. URL <https://arxiv.org/abs/2311.04036>.
- [7] M. E. J. Newman. Communities, modules and large-scale structure in networks. *Nature Physics*, 8(1):25–31, Jan 2012. ISSN 1745-2481. doi: 10.1038/nphys2162. URL <https://doi.org/10.1038/nphys2162>.
- [8] Santo Fortunato. Community detection in graphs. *Physics Reports*, 486(3):75–174, 2010. ISSN 0370-1573. doi: <https://doi.org/10.1016/j.physrep.2009.11.002>. URL <https://www.sciencedirect.com/science/article/pii/S0370157309002841>.
- [9] M. Girvan and M. E. J. Newman. Community structure in social and biological networks. *Proceedings of the National Academy of Sciences*, 99(12):7821–7826, 2002. doi: 10.1073/pnas.122653799. URL <https://www.pnas.org/doi/abs/10.1073/pnas.122653799>.
- [10] Brian Karrer and M. E. J. Newman. Stochastic blockmodels and community structure in networks. 83(1):016107. doi: 10.1103/PhysRevE.83.016107. URL <https://link.aps.org/doi/10.1103/PhysRevE.83.016107>. Publisher: American Physical Society.
- [11] Tiago P. Peixoto. *Bayesian Stochastic Blockmodeling*, chapter 11, pages 289–332. John Wiley & Sons, Ltd, 2019. ISBN 9781119483298. doi: <https://doi.org/10.1002/9781119483298.ch11>. URL <https://onlinelibrary.wiley.com/doi/abs/10.1002/9781119483298.ch11>.
- [12] Vincent D Blondel, Jean-Loup Guillaume, Renaud Lambiotte, and Etienne Lefebvre. Fast unfolding of communities in large networks. *Journal of Statistical Mechanics: Theory and Experiment*, 2008(10):P10008, oct 2008. doi: 10.1088/1742-5468/2008/10/P10008. URL <https://dx.doi.org/10.1088/1742-5468/2008/10/P10008>.
- [13] V. A. Traag, L. Waltman, and N. J. van Eck. From louvain to leiden: guaranteeing well-connected communities. *Scientific Reports*, 9(1):5233, Mar 2019. ISSN 2045-2322. doi: 10.1038/s41598-019-41695-z. URL <https://doi.org/10.1038/s41598-019-41695-z>.
- [14] M. Rosvall, D. Axelsson, and C. T. Bergstrom. The map equation. 178(1):13–23. ISSN 1951-6401. doi: 10.1140/epjst/e2010-01179-1. URL <https://doi.org/10.1140/epjst/e2010-01179-1>.
- [15] Tiago P. Peixoto. *Descriptive vs. Inferential Community Detection in Networks: Pitfalls, Myths and Half-Truths*. Elements in the Structure and Dynamics of Complex Networks. Cambridge University Press, 2023.
- [16] Tiago P. Peixoto and Alec Kirkley. Implicit models, latent compression, intrinsic biases, and cheap lunches in community detection. *Phys. Rev. E*, 108:024309, Aug 2023. doi: 10.

- 1103/PhysRevE.108.024309. URL <https://link.aps.org/doi/10.1103/PhysRevE.108.024309>.
- [17] Filippo Maria Bianchi, Daniele Grattarola, and Cesare Alippi. Spectral clustering with graph neural networks for graph pooling. URL <http://arxiv.org/abs/1907.00481>.
- [18] Rex Ying, Jiaxuan You, Christopher Morris, Xiang Ren, William L. Hamilton, and Jure Leskovec. Hierarchical graph representation learning with differentiable pooling. URL <http://arxiv.org/abs/1806.08804>.
- [19] Andrea Lancichinetti, Santo Fortunato, and János Kertész. Detecting the overlapping and hierarchical community structure in complex networks. *New Journal of Physics*, 11(3):033015, mar 2009. doi: 10.1088/1367-2630/11/3/033015. URL <https://dx.doi.org/10.1088/1367-2630/11/3/033015>.
- [20] Michael T. Schaub, Jiaze Li, and Leto Peel. Hierarchical community structure in networks. *Phys. Rev. E*, 107:054305, May 2023. doi: 10.1103/PhysRevE.107.054305. URL <https://link.aps.org/doi/10.1103/PhysRevE.107.054305>.
- [21] Tiago P. Peixoto. Hierarchical block structures and high-resolution model selection in large networks. URL <http://arxiv.org/abs/1310.4377>.
- [22] Martin Rosvall and Carl T. Bergstrom. Multilevel compression of random walks on networks reveals hierarchical organization in large integrated systems. 6(4):e18209. ISSN 1932-6203. doi: 10.1371/journal.pone.0018209. URL <https://journals.plos.org/plosone/article?id=10.1371/journal.pone.0018209>. Publisher: Public Library of Science.
- [23] Jan von Pichowski, Vincenzo Perri, Lisi Qarkaxhija, and Ingo Scholtes. Inference of sequential patterns for neural message passing in temporal graphs. URL <http://arxiv.org/abs/2406.16552>.
- [24] Christopher Blöcker, Chester Tan, and Ingo Scholtes. The map equation goes neural: Mapping network flows with graph neural networks. URL <http://arxiv.org/abs/2310.01144>. version: 3.
- [25] Tiago P. Peixoto. Nonparametric weighted stochastic block models. *Phys. Rev. E*, 97:012306, Jan 2018. doi: 10.1103/PhysRevE.97.012306. URL <https://link.aps.org/doi/10.1103/PhysRevE.97.012306>.
- [26] M. E. J. Newman. Modularity and community structure in networks. *Proceedings of the National Academy of Sciences*, 103(23):8577–8582, 2006. doi: 10.1073/pnas.0601602103. URL <https://www.pnas.org/doi/abs/10.1073/pnas.0601602103>.
- [27] Olivier Goldschmidt and Dorit S. Hochbaum. A polynomial algorithm for the k-cut problem for fixed k. *Mathematics of Operations Research*, 19(1):24–37, 1994. ISSN 0364765X, 15265471. URL <http://www.jstor.org/stable/3690374>.
- [28] Anton Tsitsulin, John Palowitch, Bryan Perozzi, and Emmanuel MÅ¼ller. Graph clustering with graph neural networks. *Journal of Machine Learning Research*, 24(127):1–21, 2023. URL <http://jmlr.org/papers/v24/20-998.html>.
- [29] Junhyun Lee, Inyeop Lee, and Jaewoo Kang. Self-attention graph pooling. URL <https://arxiv.org/abs/1904.08082v4>.
- [30] Hongyang Gao and Shuiwang Ji. Graph u-nets. URL <https://arxiv.org/abs/1905.05178v1>.
- [31] Jorma Rissanen. Modeling by shortest data description. *Automatica*, 14(5):465–471, 1978.
- [32] Peter D Grünwald, In Jae Myung, and Mark A Pitt. *Advances in minimum description length: Theory and applications*. MIT press, 2005.
- [33] Daniel Edler, Ludvig Bohlin, and Martin Rosvall. Mapping higher-order network flows in memory and multilayer networks with infomap. *Algorithms*, 10(4), 2017. ISSN 1999-4893. doi: 10.3390/a10040112. URL <https://www.mdpi.com/1999-4893/10/4/112>.
- [34] David F. Gleich. Pagerank beyond the web. *SIAM Review*, 57(3):321–363, 2015. doi: 10.1137/140976649. URL <https://doi.org/10.1137/140976649>.
- [35] Renaud Lambiotte and Martin Rosvall. Ranking and clustering of nodes in networks with smart teleportation. URL <http://arxiv.org/abs/1112.5252>.

- [36] Paul D. Dobson and Andrew J. Doig. Distinguishing enzyme structures from non-enzymes without alignments. 330(4):771–783. ISSN 0022-2836. doi: 10.1016/s0022-2836(03)00628-4.
- [37] David A. Huffman. A method for the construction of minimum-redundancy codes. *Proceedings of the IRE*, 40(9):1098–1101, 1952. doi: 10.1109/JRPROC.1952.273898.
- [38] C. E. Shannon. A mathematical theory of communication. *Bell Syst. Tech. J.*, 27:379–423, 1948.

A Map Equation Example

The map equation [6, 14, 22] is an information-theoretic objective function for community detection based on the minimum description length principle. To explain how the map equation works, we consider an undirected and unweighted network for simplicity. However, the map equation also works for directed and weighted networks.

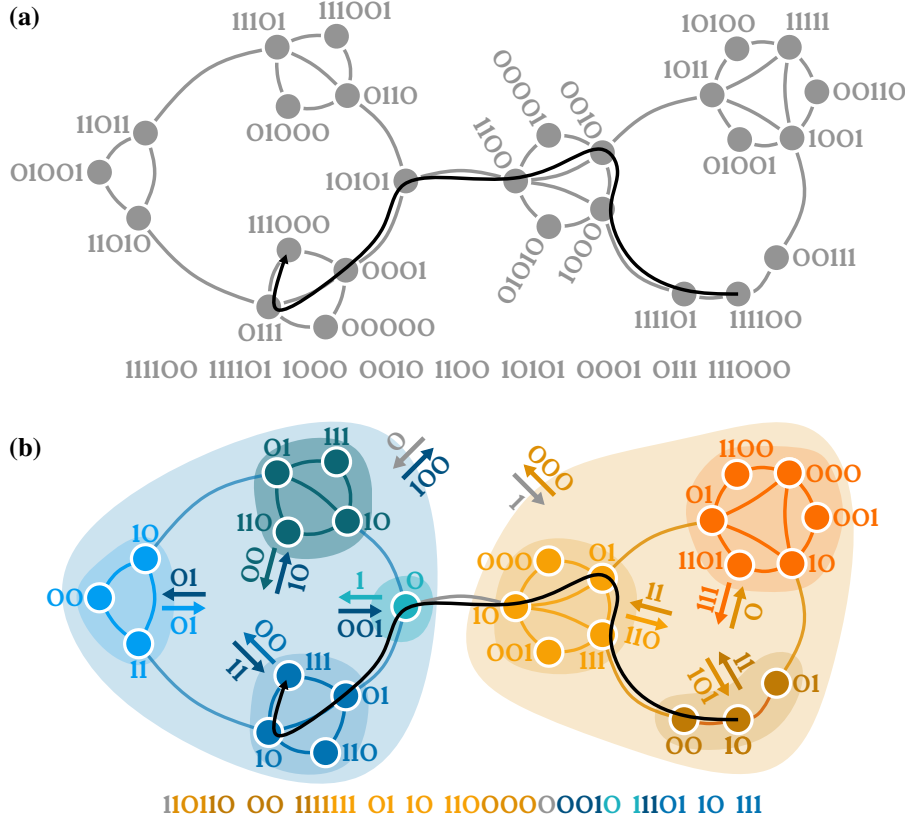


Figure 2: Coding principles behind the map equation. **(a)** All nodes are assigned to a single module and receive unique codewords. Each step of the random walker is encoded with one codeword. **(b)** The nodes are partitioned into multilevel modules as shown by colours. Now, codewords are unique within modules but the same codeword can be reused across modules, reducing the overall codeword length. One codeword is required to describe random-walker steps within modules. Steps that cross module boundaries require one additional codeword per crossed boundary, using module entry and exit codewords that are shown next to arrows pointing into and out of the modules. The black trace shows a possible sequence of random walker steps. The encoding according to the shown coding schemes is shown below the networks in (a) and (b). The codewords' colours indicate to which codebook they belong.

Consider a communication game where we describe the position of a random walker on a network $G = (V, E)$ after each step, assuming that the random walker follows links proportional to their weight. We can do this by constructing a Huffman code [37] based on the nodes' ergodic visit rates and using one codeword after each step to encode the random walker's position. In undirected networks, the visit rate of node u can be calculated in closed form as $p_u = \frac{\sum_v w_{uv}}{\sum_u \sum_v w_{uv}}$, that is, as the fraction of weight that is incident to u , where w_{uv} is the weight on the link between nodes u and v . According to Shannon's source coding theorem [38], the minimum required number of bits for describing the random walker's position is the entropy of the nodes' visit rates $P = \{p_u \mid u \in V\}$,

$$H(P) = - \sum_{u \in V} p_u \log_2 p_u.$$

Figure 2(a) shows an example network where nodes are annotated with binary codewords derived from their visit rates and a sequence of random walker steps is encoded using those codewords. We

note that, in practice, the required number of bits per random walker step—the *codelength*—can be calculated analytically as the entropy of the nodes’ visit rates.

Real-world networks often have communities, that is, groups of nodes that are more connected to each other than to the rest. To describe the position of the random walker more efficiently, nodes can be partitioned into multilevel communities, also called modules. Instead of assigning unique codewords across all nodes in the network, instead, we assign unique codewords per module. However, now that codewords are not unique anymore, we need to introduce designated module entry and exit codewords for a uniquely decodable code. With such a modular coding scheme, we use one codeword to describe steps within modules. However, when the random walker crosses module boundaries, we need to use one additional codeword for each crossed boundary, see Figure 2(b) for an example. The two-level map equation measures the codelength as a sum of weighted entropies, one per module plus one for the index level that is used to describe transitions between modules:

$$L(M) = q_{\curvearrowright} H(Q) + \sum_{m \in M} p_m^{\circlearrowleft} H(P_m).$$

The multilevel map equation generalises this approach to hierarchical partitions with more than two levels through recursion.

When minimising the map equation, two competing objectives interact. First, small modules are desirable because this leads to low module-level entropy and cheap descriptions of intra-module steps, however, creating small modules results in many modules. Second, few modules are desirable because this leads to fewer module changes, which are expensive to describe, however, only using fewer modules means creating large modules with more expensive descriptions of intra-module steps. Because these two notions are interconnected in the map equation, a tradeoff is required to minimise the random walk’s description length. In practice, these two competing objectives implement Occam’s razor and lead to automatically selecting the best number of modules across multiple levels.

B Expansion of the ℓ -level Map Equation

In the following, we present how to obtain the expanded ℓ -level map equation (eq. (3)) from the recursive definition (eq. (2)). For simplicity, we fix $\ell = 3$, however the same steps can be applied to larger ℓ . We also present a closed-form representation for an arbitrary ℓ .

We start with the recursive definition for $\ell = 3$:

$$L(M)^{(3)} = q_{\curvearrowright} H(Q) + \sum_{m^{(1)} \in M} \left[q_{m^{(1)}}^{\circlearrowleft} H(Q_{m^{(1)}}) + \sum_{m' \in m^{(1)}} q_{m'}^{\circlearrowleft} H(Q_{m'}) \right] \quad (14)$$

There are three cases to for calculating the codelength. First, the codelength for random walker transitions between top-level modules are defined as [6]:

$$H(Q) = - \sum_{m^{(1)} \in M} \frac{q_{m^{(1)}}^{\circlearrowleft}}{q_{\curvearrowright}} \log \left(\frac{q_{m^{(1)}}^{\circlearrowleft}}{q_{\curvearrowright}} \right) \quad (15)$$

Second, submodules are treated the same as their super-modules and the top-level modules but module exits need to be considered. In case of an arbitrary ℓ this definition needs to be applied repeatedly.

$$H(Q_{m^{(1)}}) = - \frac{q_{m^{(1)}}^{\circlearrowleft}}{q_{m^{(1)}}^{\circlearrowleft}} \log \left(\frac{q_{m^{(1)}}^{\circlearrowleft}}{q_{m^{(1)}}^{\circlearrowleft}} \right) - \sum_{m^{(2)} \in m^{(1)}} \frac{q_{m^{(2)}}^{\circlearrowleft}}{q_{m^{(1)}}^{\circlearrowleft}} \log \left(\frac{q_{m^{(2)}}^{\circlearrowleft}}{q_{m^{(1)}}^{\circlearrowleft}} \right) \quad (16)$$

For the lowest submodules with no further submodules the codelength is also given by the node rates.

$$H(Q_{m^{(\ell-1)}}) = - \frac{q_{m^{(\ell-1)}}^{\circlearrowleft}}{q_{m^{(\ell-1)}}^{\circlearrowleft}} \log \left(\frac{q_{m^{(\ell-1)}}^{\circlearrowleft}}{q_{m^{(\ell-1)}}^{\circlearrowleft}} \right) - \sum_{u \in m^{(\ell-1)}} \frac{p_u^{\circlearrowleft}}{q_{m^{(\ell-1)}}^{\circlearrowleft}} \log \left(\frac{p_u^{\circlearrowleft}}{q_{m^{(\ell-1)}}^{\circlearrowleft}} \right) \quad (17)$$

We obtain an expanded form of the recursive definition by inserting the previous definitions.

$$L(M)^{(3)} = -q_{\curvearrowright} \sum_{m^{(1)} \in M} \frac{q_{m^{(1)}}^{\widehat{(\cdot)}}}{q_{\curvearrowright}} \log \left(\frac{q_{m^{(1)}}^{\widehat{(\cdot)}}}{q_{\curvearrowright}} \right) \quad (18)$$

$$- q_{m^{(1)}}^{\circ} \sum_{m^{(1)} \in M} \frac{q_{m^{(1)}}^{\widehat{(\cdot)}}}{q_{m^{(1)}}^{\circ}} \log \left(\frac{q_{m^{(1)}}^{\widehat{(\cdot)}}}{q_{m^{(1)}}^{\circ}} \right) - q_{m^{(1)}}^{\circ} \sum_{m^{(1)} \in M} \sum_{m^{(2)} \in m^{(1)}} \frac{q_{m^{(2)}}^{\widehat{(\cdot)}}}{q_{m^{(1)}}^{\circ}} \log \left(\frac{q_{m^{(2)}}^{\widehat{(\cdot)}}}{q_{m^{(1)}}^{\circ}} \right) \quad (19)$$

$$- q_{m^{(2)}}^{\circ} \sum_{m^{(1)} \in M} \sum_{m^{(2)} \in m^{(1)}} \frac{q_{m^{(2)}}^{\widehat{(\cdot)}}}{q_{m^{(2)}}^{\circ}} \log \left(\frac{q_{m^{(2)}}^{\widehat{(\cdot)}}}{q_{m^{(2)}}^{\circ}} \right) - q_{m^{(2)}}^{\circ} \sum_{m^{(1)} \in M} \sum_{m^{(2)} \in m^{(1)}} \sum_{u \in m^{(2)}} \frac{p_u^{\widehat{(\cdot)}}}{q_{m^{(2)}}^{\circ}} \log \left(\frac{p_u^{\widehat{(\cdot)}}}{q_{m^{(2)}}^{\circ}} \right) \quad (20)$$

A simplification with basic logarithm rules leads to:

$$L(M)^{(3)} = - \sum_{m^{(1)} \in M} q_{m^{(1)}}^{\widehat{(\cdot)}} \log q_{m^{(1)}}^{\widehat{(\cdot)}} + \sum_{m^{(1)} \in M} q_{m^{(1)}}^{\widehat{(\cdot)}} \log q_{\curvearrowright} \quad (21)$$

$$- \sum_{m^{(1)} \in M} q_{m^{(1)}}^{\widehat{(\cdot)}} \log q_{m^{(1)}}^{\widehat{(\cdot)}} + \sum_{m^{(1)} \in M} q_{m^{(1)}}^{\widehat{(\cdot)}} \log q_{m^{(1)}}^{\circ} \quad (22)$$

$$- \sum_{m^{(1)} \in M} \sum_{m^{(2)} \in m^{(1)}} q_{m^{(2)}}^{\widehat{(\cdot)}} \log q_{m^{(2)}}^{\widehat{(\cdot)}} + \sum_{m^{(1)} \in M} \sum_{m^{(2)} \in m^{(1)}} q_{m^{(2)}}^{\widehat{(\cdot)}} \log q_{m^{(2)}}^{\circ} \quad (23)$$

$$- \sum_{m^{(1)} \in M} \sum_{m^{(2)} \in m^{(1)}} q_{m^{(2)}}^{\widehat{(\cdot)}} \log q_{m^{(2)}}^{\widehat{(\cdot)}} + \sum_{m^{(1)} \in M} \sum_{m^{(2)} \in m^{(1)}} q_{m^{(2)}}^{\widehat{(\cdot)}} \log q_{m^{(2)}}^{\circ} \quad (24)$$

$$- \sum_{m^{(1)} \in M} \sum_{m^{(2)} \in m^{(1)}} \sum_{u \in m^{(2)}} p_u^{\widehat{(\cdot)}} \log p_u^{\widehat{(\cdot)}} + \sum_{m^{(1)} \in M} \sum_{m^{(2)} \in m^{(1)}} \sum_{u \in m^{(2)}} p_u^{\widehat{(\cdot)}} \log q_{m^{(2)}}^{\circ} \quad (25)$$

We use the following definitions for the rates from the main text

$$q_{\curvearrowright} = \sum_{m^{(1)} \in M} q_{m^{(1)}}^{\widehat{(\cdot)}} \quad (26)$$

$$q_{m^{(l)}}^{\circ} = q_{m^{(l)}}^{\widehat{(\cdot)}} + \sum_{m^{(l+1)} \in m^{(l)}} q_{m^{(l+1)}}^{\widehat{(\cdot)}} \quad (27)$$

$$q_{m^{(\ell-1)}}^{\circ} = q_{m^{(\ell-1)}}^{\widehat{(\cdot)}} + \sum_{u \in m^{(\ell-1)}} p_u \quad (28)$$

to rewrite the equation further:

$$L(M)^{(3)} = - \sum_{m^{(1)} \in M} q_{m^{(1)}}^{\widehat{(\cdot)}} \log q_{m^{(1)}}^{\widehat{(\cdot)}} + q_{\curvearrowright} \log q_{\curvearrowright} \quad (29)$$

$$- \sum_{m^{(1)} \in M} q_{m^{(1)}}^{\widehat{(\cdot)}} \log q_{m^{(1)}}^{\widehat{(\cdot)}} - \sum_{m^{(1)} \in M} \sum_{m^{(2)} \in m^{(1)}} q_{m^{(2)}}^{\widehat{(\cdot)}} \log q_{m^{(2)}}^{\widehat{(\cdot)}} + \sum_{m^{(1)} \in M} q_{m^{(1)}}^{\circ} \log q_{m^{(1)}}^{\circ} \quad (30)$$

$$- \sum_{m^{(1)} \in M} \sum_{m^{(2)} \in m^{(1)}} q_{m^{(2)}}^{\widehat{(\cdot)}} \log q_{m^{(2)}}^{\widehat{(\cdot)}} - \sum_{m^{(1)} \in M} \sum_{m^{(2)} \in m^{(1)}} \sum_{u \in m^{(2)}} p_u^{\widehat{(\cdot)}} \log p_u^{\widehat{(\cdot)}} + \sum_{m^{(1)} \in M} \sum_{m^{(2)} \in m^{(1)}} q_{m^{(2)}}^{\circ} \log q_{m^{(2)}}^{\circ} \quad (31)$$

We reorder and combine the terms to the final expansion of the 3-level map equation:

$$L(M)^{(3)} = q_{\curvearrowright} \log q_{\curvearrowright} \quad (32)$$

$$+ \sum_{m^{(1)} \in M} [-q_{m^{(1)}}^{\widehat{(\cdot)}} \log q_{m^{(1)}}^{\widehat{(\cdot)}} - q_{m^{(1)}}^{\widehat{(\cdot)}} \log q_{m^{(1)}}^{\widehat{(\cdot)}} + q_{m^{(1)}}^{\circ} \log q_{m^{(1)}}^{\circ}] \quad (33)$$

$$+ \sum_{m^{(1)} \in M} \sum_{m^{(2)} \in m^{(1)}} [-q_{m^{(2)}}^{\widehat{(\cdot)}} \log q_{m^{(2)}}^{\widehat{(\cdot)}} - q_{m^{(2)}}^{\widehat{(\cdot)}} \log q_{m^{(2)}}^{\widehat{(\cdot)}} + q_{m^{(2)}}^{\circ} \log q_{m^{(2)}}^{\circ}] \quad (34)$$

$$+ \sum_{m^{(1)} \in M} \sum_{m^{(2)} \in m^{(1)}} \sum_{u \in m^{(2)}} -p_u^{\widehat{(\cdot)}} \log p_u^{\widehat{(\cdot)}} \quad (35)$$

We notice that for every new level, the equation gets expanded by the three terms found in Equation (33) or Equation (34). This observation leads to the ℓ -level expansion of the map equation $L(M)^{(\ell)}$ in Equation (3).

If we assume an undirected network

$$- \sum_{m^{(l)} \in m^{(l-1)}} q_{m^{(l)}} \log q_{m^{(l)}} = - \sum_{m^{(l)} \in m^{(l-1)}} q_{m^{(l)}} \log q_{m^{(l)}} \quad (36)$$

and a hard cluster assignment

$$- \sum_{m \in M} \sum_{m' \in m} \sum_{u \in m'} p_u \log p_u = - \sum_{u \in N} p_u \log p_u \quad (37)$$

we obtain:

$$L(M)^{(3)} = + q_{\curvearrowright} \log q_{\curvearrowright} \quad (38)$$

$$- 2 \sum_{m^{(1)} \in M} q_{m^{(1)}} \log q_{m^{(1)}} + \sum_{m^{(1)} \in M} q_{m^{(1)}}^{\circ} \log q_{m^{(1)}}^{\circ} \quad (39)$$

$$- 2 \sum_{m^{(1)} \in M} \sum_{m^{(2)} \in m^{(1)}} q_{m^{(2)}} \log q_{m^{(2)}} + \sum_{m^{(1)} \in M} \sum_{m^{(2)} \in m^{(1)}} q_{m^{(2)}}^{\circ} \log q_{m^{(2)}}^{\circ} \quad (40)$$

$$- \sum_{u \in N} p_u \log p_u \quad (41)$$

Restricting the equation to two levels leads to the map equation derived by Rosvall et al. [14]:

$$L(M) = + q_{\curvearrowright} \log q_{\curvearrowright} \quad (42)$$

$$- 2 \sum_{m \in M} q_m \log q_m + \sum_{m \in M} q_m^{\circ} \log q_m^{\circ} \quad (43)$$

$$- \sum_{u \in N} p_u \log p_u \quad (44)$$

C Losses for the Exemplary Cluster Assignments

Figure 1(a-b) presents two hierarchical cluster assignments for the same graph. The clustering-based pooling methods are guided by a loss objective. For hierarchical clustering this objective is stacked multiple times, here twice. However, we propose a hierarchical loss objective that considers both clusterings at the same time. Table 2 presents the total loss for both assignments and the loss of the fine clustering that is used to guide the first pooling layer. We note, that all stacked methods prefer the fine clustering that lead to a worse overall hierarchical clustering. The pooling operators are independent such that the worse choice is selected by the first pooling layer. However, our method selects the better hierarchical clustering because it does not consider the fine clustering on its own.

Table 2: Clustering loss for the different methods. Smaller is better. We compare the fine clustering between both examples and the hierarchical clusterings between both example.

| Method | A (fine) | B (fine) | A (hierarchical) | B (hierarchical) |
|------------------------|----------|---------------|------------------|------------------|
| DiffPool | 0.015 | 0.014 | 1.145 | 1.180 |
| MinCutPool | -0.578 | -0.600 | -1.290 | -1.267 |
| MapEqPool ^S | 3.632 | 3.548 | 5.478 | 5.605 |
| MapEqPool | - | - | 3.759 | 3.809 |

D Evaluation Details

We evaluate the models with a stratified ten-fold cross-validation. The best epoch is selected based on a validation set obtained by a 90/10% split of the training folds. The same random splits are used for all models. We apply early stopping with a patience of 100 epochs based on the classification loss for the validation set. We add ten random node features for graphs without initial features. With respect to pre-studies and common practices, we decided to use Stochastic Gradient Descent with a learning rate of 0.0001 and a batch size of 16.

All pooling functions are placed in the same model architecture to focus solely on the comparison of the pooling functions and not on the surrounding model. The model consists of three graph

convolution (GCN) layers with an embedding size of 64. Between those layers, there are the two pooling functions. The cluster assignment matrix for the baseline models is obtained through a GCN layer as presented by [18]. After the last GCN layer, the remaining nodes are pooled with global mean pooling and transformed with a linear layer to fit the classification task. We apply batch normalisation, dropout ($p = 0.5$) and ReLU as an activation function.

E Data Sets

Table 3: Properties of used data sets. The data sets vary in size and number of graphs. They contain different domains and multi- and binary classification tasks.

| Property | MUTAG | PROTEINS | COLLAB | DD | REDDIT-B | REDDIT-5K |
|----------------------|----------|----------|--------|----------|----------|-----------|
| Avg. Nodes \bar{n} | 17.93 | 39.06 | 74.49 | 284.32 | 429.63 | 508.52 |
| Graphs | 188 | 1113 | 5000 | 1178 | 2000 | 4999 |
| Classes | 2 | 2 | 3 | 2 | 2 | 5 |
| Type | Molecule | Molecule | Social | Molecule | Social | Social |

F Notes on Complexity

Our approach relies on the flow matrix [24]. The flow matrix is calculated in a pre-processing step and thus does not expand the training duration. For undirected networks, it can be calculated with a closed-form expression, however, in directed networks, it is calculated with the power iteration method where we fix the number of iterations to a constant.

During the training, for all clustering-based methods the most expensive operation is recursive pooling $\mathbf{C}_M = \mathbf{S}_M^\top \mathbf{S}_m^\top \mathbf{F} \mathbf{S}_m \mathbf{S}_M$. While we explicit state this operation, it is also present in the other methods if they are applied multiple times. It highly depends on the network sparsity and the number of modules and submodules. When $m \ll n$, $M \ll n$ and the number of edges $m = \mathcal{O}(n)$ the complexity of the pooling operator is linear. The complexity becomes quadratic when the network is dense $m = \mathcal{O}(n^2)$ or one of the cluster assignments contains nearly as many clusters as there are nodes. Even though our method strives for smaller assignments through Occam’s razor we guarantee a small number of clusters by fixing the maximum number to $M = \sqrt{n}$ and $m = \sqrt{M}$.

G Extended Empirical Evaluation

Table 4: Empirical evaluation of *MapEqPool* and five baselines with respect to different metrics.

| MUTAG | | | | |
|------------------------|---------------|---------------|-----------------|---------------|
| Method | Balanced Acc | F1 macro | Precision macro | Recall macro |
| Global Mean | 80.99 ± 10.04 | 78.28 ± 9.53 | 79.19 ± 8.47 | 80.99 ± 10.04 |
| MinCutPool | 76.13 ± 11.63 | 73.15 ± 13.84 | 72.79 ± 15.65 | 76.13 ± 11.63 |
| DiffPool | 71.72 ± 12.52 | 69.33 ± 13.68 | 70.20 ± 16.39 | 71.72 ± 12.52 |
| TopK | 63.39 ± 15.55 | 61.70 ± 17.92 | 66.78 ± 21.30 | 63.39 ± 15.55 |
| SAGPool | 75.47 ± 9.57 | 73.98 ± 9.02 | 74.81 ± 8.24 | 75.47 ± 9.57 |
| MapEqPool ^S | 79.67 ± 10.13 | 77.84 ± 9.56 | 78.29 ± 9.77 | 79.67 ± 10.13 |
| MapEqPool | 81.40 ± 6.70 | 79.38 ± 6.38 | 79.45 ± 6.84 | 81.40 ± 6.70 |
| PROTEINS | | | | |
| Method | Balanced Acc | F1 macro | Precision macro | Recall macro |
| Global Mean | 67.18 ± 4.31 | 63.80 ± 7.04 | 67.77 ± 3.87 | 67.18 ± 4.31 |
| MinCutPool | 73.10 ± 5.05 | 72.36 ± 4.86 | 72.53 ± 4.86 | 73.10 ± 5.05 |
| DiffPool | 73.22 ± 4.03 | 72.67 ± 3.73 | 72.65 ± 3.68 | 73.22 ± 4.03 |
| TopK | 65.35 ± 6.51 | 64.41 ± 5.90 | 65.09 ± 5.88 | 65.35 ± 6.51 |
| SAGPool | 62.57 ± 7.80 | 61.19 ± 11.04 | 61.74 ± 9.52 | 62.57 ± 7.80 |
| MapEqPool ^S | 71.95 ± 4.00 | 70.21 ± 3.89 | 71.47 ± 3.77 | 71.95 ± 4.00 |
| MapEqPool | 73.41 ± 4.44 | 71.62 ± 4.63 | 72.66 ± 4.59 | 73.41 ± 4.44 |
| COLLAB | | | | |
| Method | Balanced Acc | F1 macro | Precision macro | Recall macro |
| Global Mean | 64.61 ± 1.41 | 51.22 ± 3.08 | 58.63 ± 1.65 | 64.61 ± 1.41 |
| MinCutPool | 65.57 ± 3.51 | 62.22 ± 3.49 | 61.67 ± 2.96 | 65.57 ± 3.51 |
| DiffPool | 64.27 ± 3.52 | 60.77 ± 3.69 | 61.12 ± 2.93 | 64.27 ± 3.52 |
| TopK | 60.02 ± 2.72 | 51.77 ± 3.82 | 53.91 ± 2.42 | 60.02 ± 2.72 |
| SAGPool | 56.75 ± 5.07 | 49.44 ± 5.34 | 50.73 ± 4.84 | 56.75 ± 5.07 |
| MapEqPool ^S | 68.83 ± 3.55 | 64.98 ± 4.06 | 64.07 ± 4.14 | 68.83 ± 3.55 |
| MapEqPool | 65.43 ± 3.06 | 60.96 ± 3.06 | 60.65 ± 2.40 | 65.43 ± 3.06 |
| DD | | | | |
| Method | Balanced Acc | F1 macro | Precision macro | Recall macro |
| Global Mean | 69.82 ± 3.65 | 67.43 ± 5.89 | 69.93 ± 3.54 | 69.82 ± 3.65 |
| MinCutPool | 76.22 ± 2.76 | 75.90 ± 3.09 | 76.21 ± 3.10 | 76.22 ± 2.76 |
| DiffPool | 74.15 ± 4.24 | 74.20 ± 4.43 | 76.55 ± 4.95 | 74.15 ± 4.24 |
| TopK | 75.53 ± 2.79 | 75.18 ± 3.00 | 75.17 ± 3.06 | 75.53 ± 2.79 |
| SAGPool | 72.93 ± 2.39 | 72.72 ± 2.55 | 72.73 ± 2.76 | 72.93 ± 2.39 |
| MapEqPool ^S | 76.77 ± 3.06 | 76.10 ± 3.05 | 76.05 ± 3.08 | 76.77 ± 3.06 |
| MapEqPool | 78.31 ± 2.94 | 78.27 ± 3.11 | 78.34 ± 3.33 | 78.31 ± 2.94 |
| REDDIT-B | | | | |
| Method | Balanced Acc | F1 macro | Precision macro | Recall macro |
| Global Mean | 65.43 ± 3.79 | 63.76 ± 4.87 | 68.74 ± 4.76 | 65.43 ± 3.79 |
| MinCutPool | 77.28 ± 4.00 | 77.08 ± 4.13 | 77.48 ± 4.03 | 77.28 ± 4.00 |
| DiffPool | 74.48 ± 4.77 | 74.23 ± 5.03 | 74.67 ± 4.76 | 74.48 ± 4.77 |
| TopK | 77.86 ± 3.10 | 77.59 ± 3.39 | 78.76 ± 3.28 | 77.86 ± 3.10 |
| SAGPool | 79.36 ± 3.35 | 79.21 ± 3.47 | 79.67 ± 3.65 | 79.36 ± 3.35 |
| MapEqPool ^S | 77.60 ± 2.80 | 77.38 ± 2.92 | 78.23 ± 3.01 | 77.60 ± 2.80 |
| MapEqPool | 77.74 ± 3.49 | 77.65 ± 3.54 | 78.19 ± 3.79 | 77.74 ± 3.49 |
| REDDIT-5K | | | | |
| Method | Balanced Acc | F1 macro | Precision macro | Recall macro |
| Global Mean | 36.99 ± 4.65 | 29.84 ± 7.58 | 35.92 ± 7.16 | 36.99 ± 4.65 |
| MinCutPool | 47.14 ± 1.69 | 44.23 ± 2.21 | 46.92 ± 2.33 | 47.14 ± 1.69 |
| DiffPool | 47.54 ± 2.11 | 45.21 ± 2.15 | 46.33 ± 2.45 | 47.54 ± 2.11 |
| TopK | 47.65 ± 2.24 | 45.69 ± 2.45 | 46.07 ± 2.58 | 47.65 ± 2.24 |
| SAGPool | 45.54 ± 2.88 | 43.71 ± 3.30 | 43.78 ± 3.29 | 45.54 ± 2.88 |
| MapEqPool ^S | 45.65 ± 3.64 | 43.19 ± 4.75 | 44.67 ± 4.71 | 45.65 ± 3.64 |
| MapEqPool | 46.86 ± 1.80 | 43.89 ± 2.76 | 45.51 ± 2.09 | 46.86 ± 1.80 |